

# BOREHOLE STONELEY WAVE PROPAGATION ACROSS PERMEABLE STRUCTURES: COMPARISON BETWEEN THEORY AND EXPERIMENT

by

Zhenya Zhu, Xiaoming Tang\*, C.H. Cheng, and M.N. Toksöz

Earth Resources Laboratory  
Department of Earth, Atmospheric, and Planetary Sciences  
Massachusetts Institute of Technology  
Cambridge, MA 02139

\*NER Geoscience  
1100 Crown Colony Drive  
Quincy, MA 02169

## ABSTRACT

The attenuation of borehole Stoneley waves across a permeable structure (e.g., fractures or fracture zone) is correlated with the permeability of the structure. Using a simplified Biot theory, the structure can be modelled as a permeable porous layer intersecting the borehole. In order to study the effect of such a structure on Stoneley waves and to evaluate the theoretical model, we performed laboratory experiments using ultrasonic borehole models. The porous layer model is made of fine-grained sands with high permeability and porosity. The experiments are carried out with three saturant fluids: water, alcohol, and glycerol. The iso-offset Stoneley waveforms are recorded by moving the source and receiver across the porous layer. In this way, robust estimates of Stoneley wave transmission coefficients are obtained. The experimental transmission coefficients are compared with the theoretical coefficients calculated using the borehole and permeable zone parameters. There is good agreement between theoretical results and experimental results. For low viscosity fluid water and ethyl alcohol, the agreement is very good. For high viscosity fluid, glycerol, the agreement is fair with the experimental Stoneley attenuation higher than the theoretical value.

## INTRODUCTION

Permeable fractures in reservoirs are of major significance in assessing the fluid transport properties in the production of petroleum. Permeable fractures are also important in

waste disposal siting studies and in environmental geophysics, as well as ground water transport. Through field observations, Paillet (1980) was able to recognize the effect of fractures intersecting the borehole on full wave acoustic logging waveforms. The low frequency Stoneley waves are especially sensitive to the formation permeability and fluid transportation, and they have been used as important means in the detection and characterization of borehole fractures.

Paillet and White (1982) observed that the borehole Stoneley wave attenuates across permeable fractures. Hornby et al. (1989) showed that permeable fractures also give rise to reflected Stoneley waves. Theoretical studies (Stephen et al., 1985; Tang, 1990; Kostek, 1991) have been carried out to model the effects of a borehole fracture. In all these models, the analogy of a parallel planar fluid layer was commonly adopted to represent the fracture. Although both the attenuation and the reflection of the Stoneley wave are predicted by the plane-fracture model, it takes a rather large fracture aperture (on the order of centimetres) to produce significant Stoneley wave attenuation. However, fractures with such apertures are rarely found in the field (Hornby et al., 1989), but Stoneley wave attenuation of up to 50% or more across in situ fractures is commonly observed (Paillet, 1980; Hardin et al., 1987). Paillet (1989) suggested that in situ fractures may consist of an array of low passages and that fracture permeability is not directly related to the apertures of a plane-parallel fracture. Tang and Cheng (1991) explicitly modeled the borehole fractures as a permeable porous zone, in which a simplified Biot-Rosenbaum theory (Tang et al., 1991a) was used to calculate the effect of the porous zone. Using this model, they investigated the propagation of borehole Stoneley waves across a permeable fracture zone. The results show that strong Stoneley wave attenuation is produced across the permeable zone. Although the model seemed to explain some field data sets fairly well (Tang et al., 1991b), its accuracy and validity have not been tested with a controlled experiment. Through laboratory experiments, Winkler (1989) verified the validity of the Biot-Rosenbaum theory of Stoneley wave propagation in a porous formation. The purpose of this study is to test the validity and applicability of the simplified Biot-Rosenbaum theory of Tang et al. (1991a) to the modeling of Stoneley wave propagation across permeable fractures.

Laboratory experiments with fluid-filled plane fracture models were performed in recent years (Hornby et al., 1989; Güler and Toksöz, 1987; Poeter, 1987; Zlatev et al., 1988). The attenuation of the Stoneley wave was measured using the ultrasonic models with horizontal or inclined fluid-filled fractures of various apertures. In these experiments, the acoustic source was fixed, and the receiver was moved across the fracture along the borehole. The array waveforms were recorded. It has been shown that the amplitude attenuation of waveforms is related to the apertures of the fractures. In the present study, the source and receiver spacing is fixed and the assembly is moved across the permeable zone. This geometry is adopted to simulate the iso-offset configuration in an acoustic logging measurement.

This study investigates the propagation of Stoneley waves across a permeable porous zone in an ultrasonic model. Parameters such as porosity, permeability, and P- and S-wave velocities of the material of the zone are independently measured. These parameters will be used in the theoretical model to calculate Stoneley wave propagation and the results will be compared with the experimental results. To perform the experiments, a pair of transducers for use in the ultrasonic model borehole are built using piezoelectric rings. The received waveforms are recorded with a digital oscilloscope to measure the effect of permeable zone. The transmission coefficient of the Stoneley wave across the fracture is calculated and is compared with the theoretical one. This comparison offers a test of the validity of the theory.

## ULTRASONIC MODEL AND MEASUREMENT SYSTEM

In the previous ultrasonic borehole models with fracture (Hornby et al., 1987), a horizontal fluid-filled gap was used to simulate the fracture. The primary interest of the present study is to model the fracture as a permeable zone sandwiched between two impermeable solids.

To simulate the iso-offset downhole acoustic logging commonly used in the field, we have built a laboratory logging tool that consists of source and receiver transducers made from piezoelectric rings of small diameter. The source and receiver can move in the model borehole with fixed or variable spacing to measure waveforms across the permeable structure.

### Ultrasonic Model

Quartz sands with grain diameters ranging from 0.5 to 0.8 mm are used to construct the synthetic porous permeable material. The sands are mixed with a low-viscosity glue (Ladd ultra-low viscosity embedding medium #21220) at room temperature, and are shaped into cylinder and disk samples. The shaped samples are cured at 70°C temperature for 8 hours. The physical parameters of the samples are then measured and later used in the theoretical modelling.

The compressional and shear velocities are measured with the dry cylinder sample. They are 2510 m/s and 1420 m/s, respectively. Then the sample is fully saturated with water. The weights of the sample before and after water saturation, and the weight of the sample suspended in water, are then measured. The densities of grain matrix and the water-saturated sample are  $2.50\text{g/cm}^3$  and  $1.96\text{g/cm}^3$ , respectively. From the densities, the porosity of the sample is estimated to be 36.1 %. The permeability is measured by means of the steady-state flow method with the setup shown in Figure 1. A constant pore pressure gradient is applied across the sample and the volume of fluid

flowing through it per unit time is measured. The permeability  $\kappa$  is given by Darcy's law:

$$\kappa = \frac{\mu \Delta W \Delta x}{\rho^2 g H \Delta t \Delta A} \quad (1)$$

where  $\mu$  is the water viscosity (1.002 centipoise),  $\Delta A$  is the cross-sectional area of the sample,  $\rho$  the water density,  $\Delta W$  the mass of water flowing through the sample of length  $\Delta x$  in the time interval  $\Delta t$ ,  $H$  the height difference of water surfaces shown in Figure 1, and  $g$  is the gravitational acceleration (i.e., 980  $cm/sec^2$ ).

In our experiment, the height difference was 19.6 cm, the water mass through the cylinder sample of diameter 3.15 cm and length 4.0 cm in the time interval of 90 seconds was 385 gram. Therefore, the permeability is estimated to be 126 darcy ( $10^{-8} cm^2$ ) for the synthetic porous material.

The man-made porous disk has a thickness of 1.15 cm. A borehole of 1 cm diameter was drilled at its center. The ultrasonic borehole model with a permeable structure was constructed by sandwiching the disk between two aluminum cylinders. The cylinders have an outer diameter of 20.3 cm and height of 15.2 cm. The center of the cylinder was drilled to make a borehole of 1 cm diameter. The various parameters of the borehole model are given in Table 1.

## Transducers

A pair of transducers, one source and one receiver, are made of piezoelectric rings. The rings have an outer radius of 0.35 cm, inner radius of 0.14 cm, and height of 0.7 cm. When excited by an electric pulse, the rings vibrate primarily in the radial direction. Each ring was sealed by silicon rubber (Flexane resin) to form a single transducer, which has a diameter of 0.83 cm. A downhole tool is assembled by connecting two single transducers with a fine steel wire (Figure 2). The distance between source and receiver is 6.1 cm. During the experiment, the assembly shown in Figure 2 is placed in the borehole model to simulate the iso-offset acoustic logging in the field.

The frequency response of a single transducer was measured in a water tank. The experiment shows that the transducer has good response down to 30 kHz. When placed in the borehole, the borehole will change the excited and received signals of the transducers. Because the diameter of the tool is only slightly smaller than that of borehole (0.83 cm vs. 1 cm), the cut-off frequencies of the borehole pseudo-Rayleigh waves will be shifted to very high frequencies. Even at fairly high frequencies (up to 350 kHz), the received waveform consists primarily of Stoneley waves. Therefore, this design of ultrasonic transducers is especially suited for generating and receiving Stoneley waves.

## Experimental Setup

The block diagram of the experimental setup is shown in Figure 3. A function generator produces a sync-trigger signal to activate a high-voltage pulse generator. The source is driven by a sharp pulse and emits acoustic waves in the fluid-filled borehole. The waves propagating along the borehole are received and converted into electrical signals by the receiver transducer. The signals are first amplified and filtered. Then the signals are digitized by a digital oscilloscope (Data Precision 6000). The digital waveforms are stored in an IBM/AT or transferred to the VAX 8800 for further analysis. The transducers are mounted on a frame which can be moved step by step by a step motor controller along the borehole. The microseismograms can be recorded at different locations in the model borehole.

## MEASUREMENTS IN THE MODEL

To test the ultrasonic measuring system, we performed the measurement in a homogeneous aluminum model, using the variable source-receiver spacing configuration. Figure 4 shows the array waveforms obtained for this configuration.

The center frequency of the signals is about 250 kHz, which is above the cut-off frequency (about 170 kHz) of the first pseudo-Rayleigh mode for the fluid-filled 1 cm diameter aluminum borehole. However, because the borehole transducer has a diameter that is only slightly smaller than the borehole diameter, the pseudo-Rayleigh waves are not excited in this frequency range, and the received waves are dominated by Stoneley waves. This can be seen by measuring the moveout velocity of the waveforms, which is the Stoneley wave velocity (1450 m/s). The microseismograms also show that the other wave modes (such as P-Leaky modes) are suppressed by the transducer used.

The ultrasonic measurements were carried out to study the effect of the permeable layer on the Stoneley waves. To test the theoretical model, we use three saturant fluids with very different physical properties. They are water, ethyl alcohol and glycerol. The physical properties of these fluids are given in Table 2.

## RESULTS AND DISCUSSION

From the recorded microseismograms, the average amplitude of Stoneley waves of each trace can be computed. This amplitude is calculated as the square root of the sum of the squared amplitudes of the waveforms. The plot of the amplitudes across the porous layer gives a robust estimate of the Stoneley wave transmission coefficient across the layer (Tang et al., 1991b).

We first show the theoretical and experimental results for the water-saturated porous layer. Figure 5a shows the recorded iso-offset waveforms and the calculated wave amplitudes. The Stoneley waves propagate across the porous layer; the amplitudes are appreciably decreased by the layer, due to the dissipation of wave energy into the permeable layer. Figure 5b shows the theoretical modelling results. The results are calculated using the Tang and Cheng (1991) theory with the parameters given in Tables 1 and 2. The theory, together with a correction due to the finite vertical extent of the permeable zone, is described in the Appendix. The theoretical waveforms show the characteristic amplitude decrease across the permeable zone, as we have seen in Figure 5a. In addition, there are reflected waves generated by the zone. However, the reflected waves cannot be measured with the transducers shown in Figure 1, because the small fluid annulus at the receiver will cause the generated (small) reflection events to be largely reflected away from the receiver. Therefore, we can only rely on the transmitted waves. The amplitude log at the edges of the anomaly is considerably smaller than in the central part of the anomaly. This is also true for the following two examples. This happens when either the source or receiver is within the permeable zone. Because the zone is much softer than the surrounding (aluminum) model, the excited (or received) waves are much weaker than when the source or receiver is outside the zone. Therefore, only the central part of the amplitude anomaly is used to measure the transmitted amplitude, from which the transmission coefficient is calculated as the ratio of the transmitted amplitude over the incident amplitude. The comparison between the theoretical transmission coefficient and the experimental coefficient obtained for the frequency of measurement is shown in Figure 5a for the water-saturated case. The agreement is excellent.

In the second example, we compare the theoretical and experimental results for the ethyl alcohol, which was used to saturate the porous layer and fill the borehole during the experiment. The results are shown in Figures 6a and 6b. Because of the low velocity of ethyl alcohol, the arrival of Stoneley waves is significantly delayed compared to the water-saturation case in Figure 5a. The synthetic waveforms across the porous layer agree with the measured waveforms very well. The amplitude log calculated from the synthetic waveform fits the measured log excellently (see also Figure 6b).

The third example is for a highly viscous saturant fluid glycerol ( $\mu=1490$  cp). Both the measured waveform (280 kHz center frequency) and the experimental amplitude log (Figure 7a) show amplitude decrease across the porous layer. The theoretical attenuation value (Figure 7b) of 0.5 is close to but higher than the experimental value (0.43). In this case, the theory underestimates the experimental transmission loss across the porous layer. This discrepancy could be due to the high viscosity value of the fluid and may imply that if a reservoir is saturated with very viscous hydrocarbons, the Stoneley wave attenuation may be higher than the simplified Biot's theory predictions.

## CONCLUSIONS

We have established an experimental procedure for measuring Stoneley wave propagation across permeable structures in the laboratory borehole models. With controlled model parameters, we evaluated the applicability of simplified Biot's theory to the modelling of a permeable structure intersecting the borehole. This theory gives satisfactory results for low viscosity fluids like water and ethyl alcohol. For a highly viscous fluid such as glycerol, the Stoneley wave exhibits more attenuation than the theory predicts. In general, the theory and experiment agree fairly well. The experiment validates the theory as a useful model for calculating Stoneley wave propagation across a permeable zone.

## ACKNOWLEDGEMENTS

This research was supported by the Borehole Acoustics and Logging Consortium at M.I.T. and Department of Energy grant DE-FG02-86ER13636.

## REFERENCES

- Biot, M.A., 1956a, Theory of propagation of elastic waves in a fluid-saturated porous solid, I: low frequency range, *J. Appl. Phys.*, *33*, 1482–1498.
- Biot, M.A., 1956b, Theory of propagation of elastic waves in a fluid-saturated porous solid, II: Higher frequency range, *J. Acoust. Soc. Am.*, *28*, 168–178.
- Cheng, C.H., J. Zhang, and D.R. Burns, 1987, Effects of in-situ permeability on the propagation of Stoneley (tube) waves in a borehole, *Geophysics*, *52*, 1297–1289.
- Güler, F., and M.N. Toksöz, 1987, Ultrasonic laboratory study of full waveform acoustic logs in boreholes with fractures, *M.I.T. Full Waveform Acoustic Logging Consortium Annal Report*.
- Hardin, E.L., C.H. Cheng, F.L. Paillet, and J.D. Mendelson, 1987, Fracture characterization by means of attenuation and generation of tube waves in fractured crystalline rock at Mirror Lake, New Hampshire, *J. Geophys. Res.*, *92*, 7989–8006.
- Hornby, B.E., D.L. Johnson, K.H. Winkler, and R.A. Plumb, 1989, Fracture evaluation using reflected Stoneley-wave arrivals, *Geophysics*, *54*, 1274–1288.
- Johson, D.L., J. Koplik, and R. Dashen, 1987, The theory of dynamic permeability and tortuosity in fluid-saturated porous media, *J. Fluid Mech.*, *173*, 379–400.
- Kostek, S., 1991, Borehole acoustic wave propagation in the presence of fractures: a finite difference approach, *SEG 61st Annual International Meeting, Expanded Abstracts*, 863–866.
- Paillet, F.L., 1980, Acoustic propagation in the vicinity of fractures which intersected a fluid-filled borehole, *Trans., SPWLA 21st Ann. Symp.*, paper DD.
- Paillet, F.L., and J.E. White, 1982, Acoustic modes of propagation in the borehole and their relationship to rock properties, *Geophysics*, *47*, 1215–1228.
- Paillet, F.L., C.H. Cheng, and X.M. Tang, 1989, Theoretical models relating acoustic tube-wave attenuation to fracture permeability-reconciling model results with field data, *Trans. SPWLA 30th Annl. Symp.*, paper FF.
- Poeter, E.P., 1987, Characterizing fractures at potential nuclear waste repository sites with acoustic waveform logs, *The Log Analyst*, 453–461.
- Stephen, D.P., F. Pardo-Casas, and C.H. Cheng, 1985, Finite difference synthetic acoustic logs, *Geophysics*, *50*, 1588–1609.
- Tang, X.M., and C.H. Cheng, 1988, A dynamic model for fluid flow in open borehole



- fracture, *J. Geophys. Res.*, *94*, 7567–7576.
- Tang, X.M., 1990, Acoustic logging in fractured and porous formations, Sc.D Thesis, Massachusetts Institute of Technology, Cambridge, MA.
- Tang, X.M., and C.H. Cheng, 1991, Borehole Stoneley wave propagation across heterogeneous and permeable structures, *M.I.T. Full Waveform Acoustic Logging Consortium Annual Report*.
- Tang, X.M., C.H. Cheng, and M.N. Toksöz, 1991a, Dynamic permeability and borehole Stoneley waves: A simplified Biot–Rosenbaum model, *J. Acous. Soc. Am.*, *90*, 1632–1646.
- Tang, X.M., C.H. Cheng, and F.L. Paillet, 1991b, Modelling Stoneley wave propagation across in-situ fractures, *Trans. 36th Soc. Prof. Well Log Analysts*.
- White, J.E., 1983, *Underground Sound*, Elsevier Science Publishing Co. Inc.
- Winkler, K.W., H.L. Liu, and D.L. Johnson, 1989, Permeability and borehole Stoneley waves: Comparison between experiment and theory, *Geophysics*, *54*, 66–75.
- Zlatev, P., E. Poeter, and J. Higgins, 1988, Physical modeling of the full acoustic waveform in a fractured, fluid-filled borehole, *Geophysics*, *53*, 1219–1224.

## Appendix A. THEORY OF STONELEY WAVE PROPAGATION ACROSS A PERMEABLE ZONE

In this appendix, we describe the theory of Stoneley wave propagation across a permeable borehole structure. A modification of the original theory of Tang and Cheng (1991) is also presented.

Consider a horizontal permeable zone of thickness  $L$  sandwiched between two non-permeable formations. In order to describe the wave characteristics in the borehole section  $0 < z < L$ , we use the equation of mass conservation for a small amplitude wave motion (Tang and Cheng, 1989)

$$i\omega \oint_S \vec{U} \cdot d\vec{S} = \frac{i\omega}{\rho_f V_f^2} \int_{\nabla V} -p dv \quad (\text{A-1})$$

where  $\vec{U}$  is the fluid displacement,  $\rho_f$  is fluid density,  $V_f$  is fluid acoustic velocity,  $p$  is pressure;  $\omega$  is angular frequency,  $\nabla V = \pi R^2 L$  ( $R$ =bore radius) is the volume of the borehole section located at the permeable zone, and  $S$  is the surface enclosing  $\nabla V$ . Eq. (A-1) means that the dynamic volume compression of  $\nabla V$  equals the net fluid flux into  $\nabla V$ . The axial flux can be easily calculated. At  $z=0$ , the flux is  $i\omega U_z(0)\pi R^2$ . At  $z=L$ , it is  $-i\omega U_z(L)\pi R^2$ , where  $U_z$  is the axial displacement. In the radial direction, the displacement includes two contributions (Tang et al., 1991a). The first is the displacement of the equivalent elastic formation without flow, given by  $U_e$ . The second is the fluid flow into the permeable formation, given by  $\phi U_f$ , where  $\phi$  is the porosity of the zone. With these quantities specified, Eq. (A-1) can be written as

$$[U_z(L) - U_z(0)] \cdot \pi R^2 + [U_e + \phi U_f] \cdot 2\pi RL = \frac{\pi R^2 L}{\rho_f V_f^2} p. \quad (\text{A-2})$$

Dividing Eq.(A-2) by  $\pi R^2 L$  and using

$$U_z = \frac{1}{\rho_f \omega^2} \frac{dp}{dz},$$

and the approximation

$$\frac{U(L) - U(0)}{L} \approx \frac{dU}{dz},$$

we obtain a wave equation for the borehole pressure in the  $0 < z < L$  region, given as

$$\frac{d^2 p}{dz^2} + \left[ \frac{\omega^2}{V_f^2} + \frac{2\rho_f \omega^2}{R} \left( \frac{U_e}{p} + \frac{\phi U_f}{p} \right) \right] p = 0. \quad (\text{A-3})$$

Without fluid flow (i.e.,  $U_f = 0$ ), Eq.(A-3) describes the Stoneley wave propagation in the equivalent elastic formation with a wave number

$$k_e = \sqrt{\frac{\omega^2}{V_f^2} + \frac{2\rho_f\omega^2}{R} \cdot \frac{U_e}{p}}. \quad (\text{A-4})$$

At low frequencies,  $\frac{U_e}{p} = \frac{R}{\rho V_s^2}$  (White, 1983), thus we see that  $k_e = \frac{\omega}{C_T}$ , where  $C_T = \frac{V_f}{\sqrt{1 + \frac{\rho_f V_f^2}{\rho V_s^2}}}$  is the low frequency tube wave velocity,  $\rho$  and  $V_s$  are formation density and shear velocity, respectively. At high frequencies,  $k_e$  is approximately the Stoneley wave number calculated using the equivalent formation properties (Tang et al., 1991a). This approximation is due to the 1-D simplification used here.

We now calculate the flow  $U_f$  into the permeable zone. Outside the borehole into the porous zone, the equation governing the dynamic fluid flow pressure  $P$  is (Tang et al., 1991a)

$$\frac{\partial^2 P}{\partial r^2} + \frac{1}{r} \frac{\partial P}{\partial r} + \frac{\partial^2 P}{\partial z^2} + \frac{i\omega}{D} P = 0 \quad (r \geq R, 0 < z < L) \quad (\text{A-5})$$

where

$$D = \frac{\kappa(\omega)\rho_f V_f^2}{\phi\mu(1+\xi)}$$

is the pore fluid diffusivity,  $\mu$  is viscosity,  $\xi$  is a correction for pore matrix compressibility (see Tang et al., 1991a), and  $\kappa(\omega)$  is the dynamic permeability (Johnson et al., 1987)

The solution to Eq.(A-5) is found to be

$$P = \sum_{n=0}^{\infty} \frac{K_0(r\sqrt{-i\omega/D + k_n^2})}{K_0(R\sqrt{-i\omega/D + k_n^2})} [P_n \cos k_n z + q_n \sin k_n z] \quad (\text{A-6})$$

where  $K_0$  is the modified Bessel function,  $P_n$  and  $q_n$  are Fourier expansion coefficients, and  $k_n$ 's are the vertical wave numbers in the zone, which can be specified by boundary conditions at  $z=0$  and  $z=L$ . The fluid flow is given by the modified Darcy's law (Tang et al., 1991)

$$-i\omega\phi\bar{U}_f = -\frac{\kappa(\omega)}{\mu}\nabla P.$$

Due to the assumption that the permeable zone is sandwiched between two impermeable formations, the vertical flow  $U_{fz} = \frac{\kappa(\omega)}{i\omega\phi\mu} \frac{\partial P}{\partial z}$  should be zero at  $z=0$  and  $z=L$ . Computing  $\frac{\partial P}{\partial z}$  using Eq. (A-6) results in

$$q_n = 0,$$

and

$$k_n = \frac{n\pi}{L} \quad (n = 0, 1, 2, 3, \dots).$$

The radial flow  $U_f = \frac{\kappa(\omega)}{i\omega\phi\mu} \frac{\partial P}{\partial z} |_{r=R}$  can also be calculated using Eq.(A-6). Averaging  $U_f$  over  $0 < z < L$ , we see that all the  $n > 0$  terms in Eq.(A-6) vanish and only the  $n = 0$  term contributes to the average flow, with  $P_0$  equal to the borehole pressure  $P$  in the  $0 < z < L$  region. This gives the average flow

$$U_f = P \cdot \frac{iK\kappa(\omega)}{\omega\mu\phi} \sqrt{-i\omega/D} \frac{K_1(R\sqrt{-i\omega/D})}{K_0(R\sqrt{-i\omega/D})}. \quad (\text{A-7})$$

Substituting Eq. (A-7) into the wave equation (Eq. A-3), we see that the Stoneley wave propagation in the permeable zone is characterized by a wave number

$$k = \sqrt{k_e^2 + \frac{2i\rho_f\omega\kappa(\omega)}{\mu R} \sqrt{\frac{-i\omega}{D}} \frac{K_1(R\sqrt{-i\omega/D})}{K_0(R\sqrt{-i\omega/D})}}. \quad (\text{A-8})$$

In the original theory of Tang and Cheng (1991), the term  $\sqrt{-i\omega/D}$  was  $\sqrt{-i\omega/D + k_e^2}$ , where  $k_e$  was due to coupling of the formation fluid flow with the borehole propagation in a borehole of infinite extent (Tang et al., 1991a). The elimination of  $k_e$  in the present case means that the flow in the permeable zone is primarily in the radial direction and does not couple with the borehole propagation, because of the limited vertical extent of the zone. We point out that this correction is not significant in the low frequency range where  $\omega/D \gg k_e$ . Only at high frequencies where  $i\omega/D$  becomes  $k_{slow}^2$  (where  $k_{slow}$  is the Biot's (1956b) slow wave number at high frequencies), will this correction have some measurable effects.

Once the wave number  $k$  in the permeable zone is found, the Stoneley wave transmission and reflection coefficients TC and RC are calculated using (Tang and Cheng, 1991)

$$TC = \frac{4k_1 k e^{-ikL}}{(k_1 + k)^2 e^{-ikL} - (k_1 - k)^2 e^{ikL}} \quad (\text{A-9})$$

$$RC = \frac{2i(k^2 - k_1^2) \sin(kL)}{(k_1 + k)^2 e^{-ikL} - (k_1 - k)^2 e^{ikL}} \quad (\text{A-10})$$

where  $k_1$  is the Stoneley wave number outside the  $0 < z < L$  region.

Table 1: Physical parameters of the ultrasonic borehole model, the value of tortuosity  $\alpha(=2.4)$  is taken from Winkler et al. (1989) for a synthetic porous medium.

Medium	P-wave $V_p(\text{dry})$ (m/s)	S-wave $V_s(\text{dry})$ (m/s)	Density $\rho$ (kg/m <sup>3</sup> )	Compressibility $K_s(Gp\omega)$	Porosity $\phi$ $\phi(\%)$	Permeability $\kappa(\text{darcy})$	Tortuosity $\alpha$
Synthetic Porous Layer	2510	1420	2500	37.9	36.1	126	2.4
Aluminum	6400	3100	2700	–	–	–	–

Table 2: Saturant fluid properties

Fluid	Velocity V (m/s)	Density $\rho(\text{kg/m}^3)$	Viscosity (cp)
Water	1480	1000	1.002
Alcohol	1130	790	1.2
Glycerol	1820	1260	1490

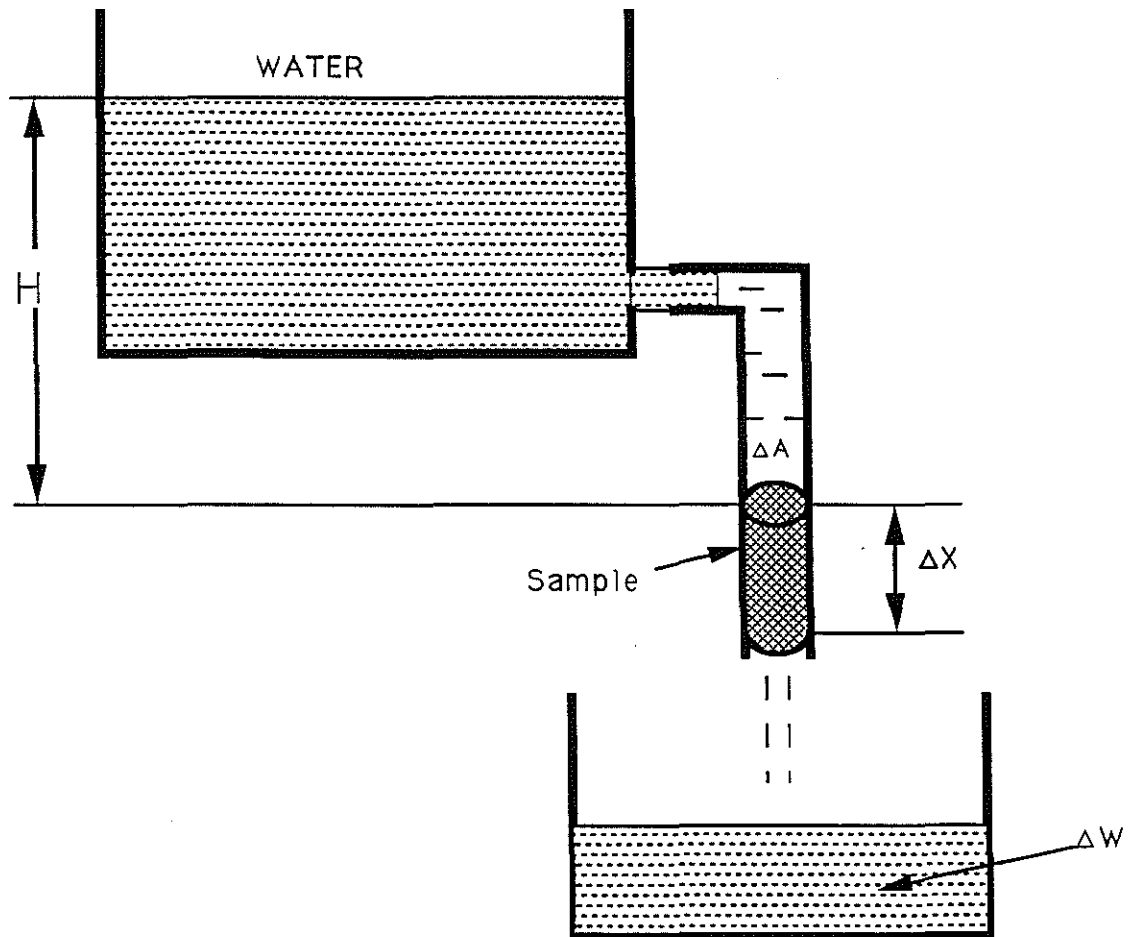


Figure 1: A diagram of experiment designed to measure the permeability of a sample with steady-state flow method.

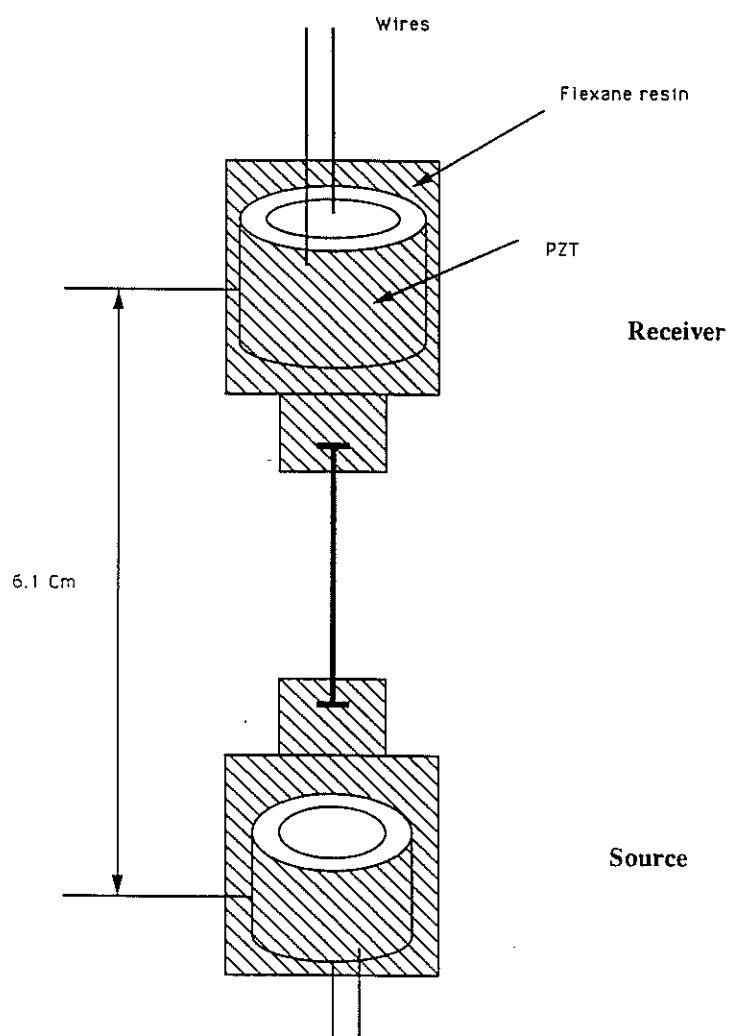


Figure 2: Schematic diagram of the source-receiver pair made of PZT piezoelectric rings. The outside diameter of the transducers is 0.83 cm.

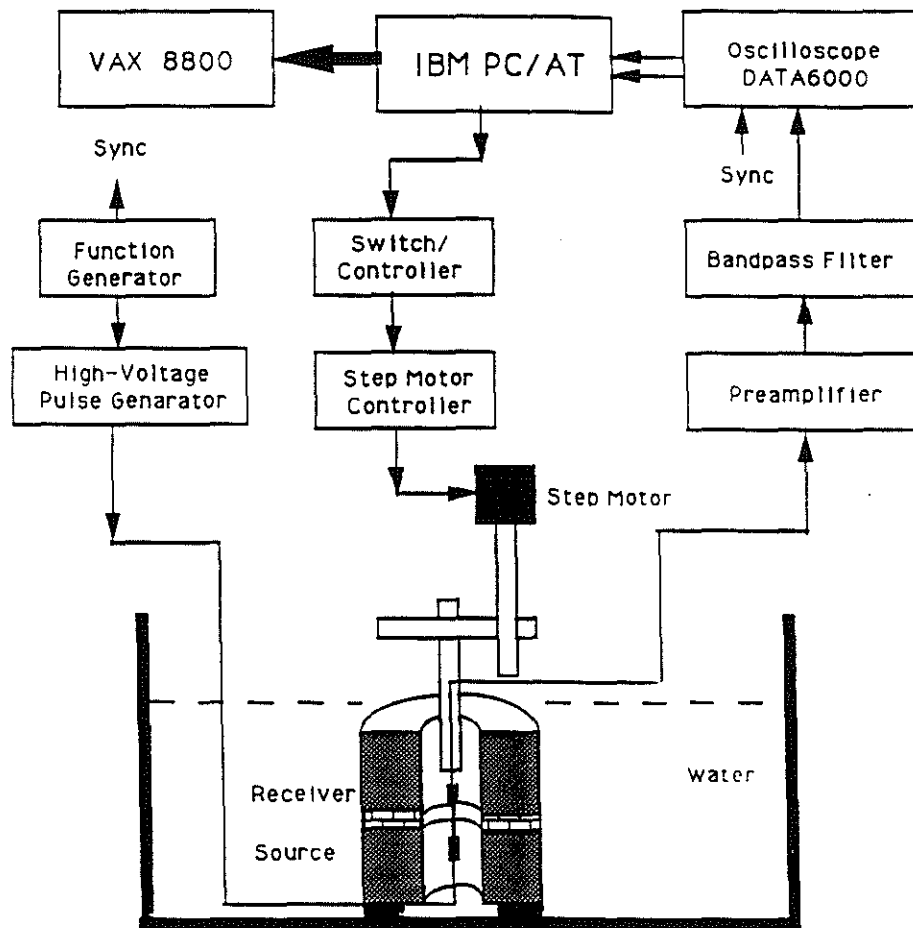


Figure 3: Block diagram of experiment setup.



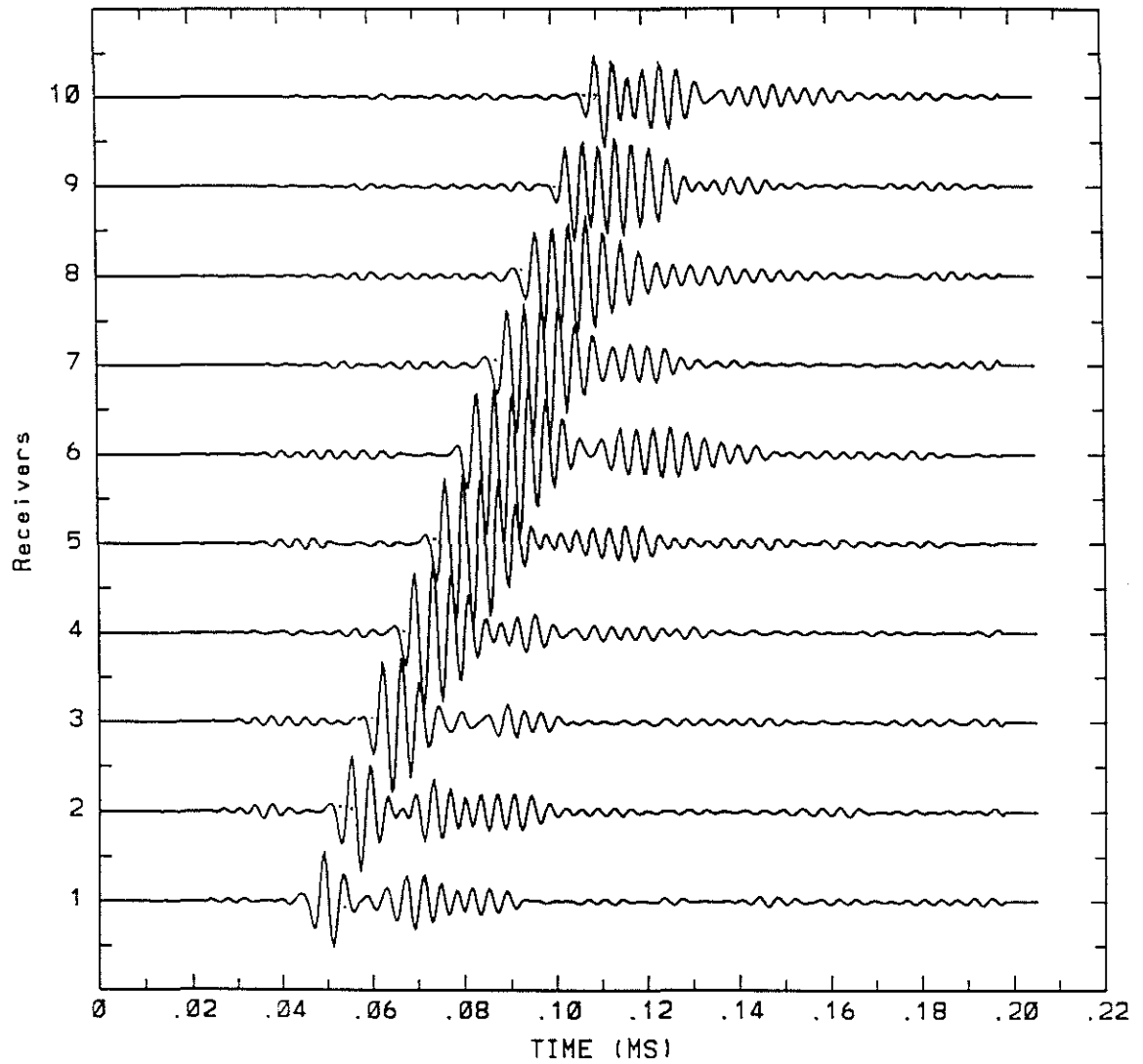


Figure 4: Waveforms recorded in an intact aluminum model at varying source-receiver spacing of 1.0 cm. The center frequency of the signals is about 250 kHz.

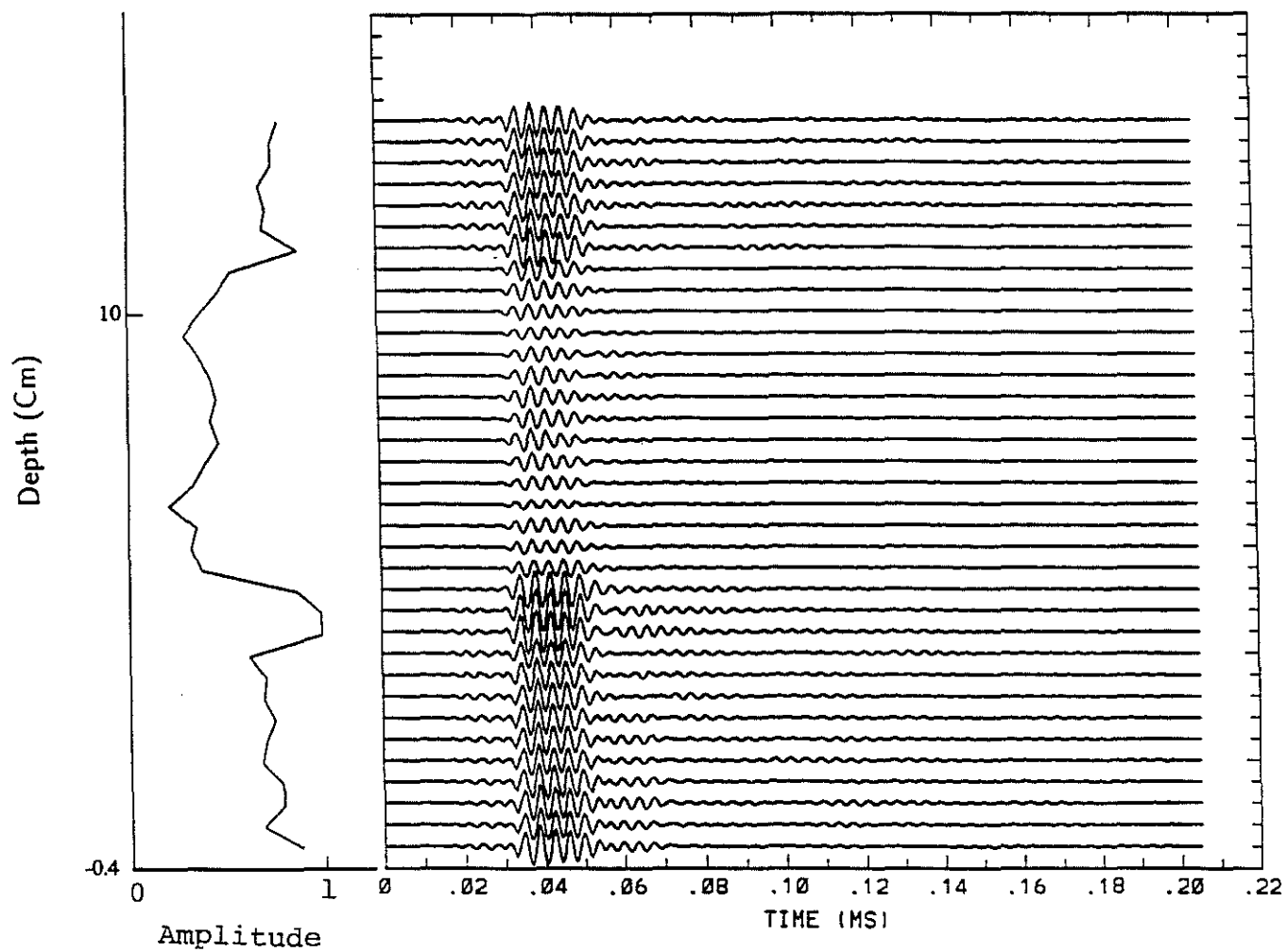


Figure 5: a) Amplitude of Stoneley waves and waveforms recorded (depth increment=0.4 cm) in a permeable zone borehole model saturated with water. The width of the permeable zone is 1.15 cm. The porosity and permeability are 36.1 % and 126 darcy respectively. The measured transmission coefficient is 0.52.

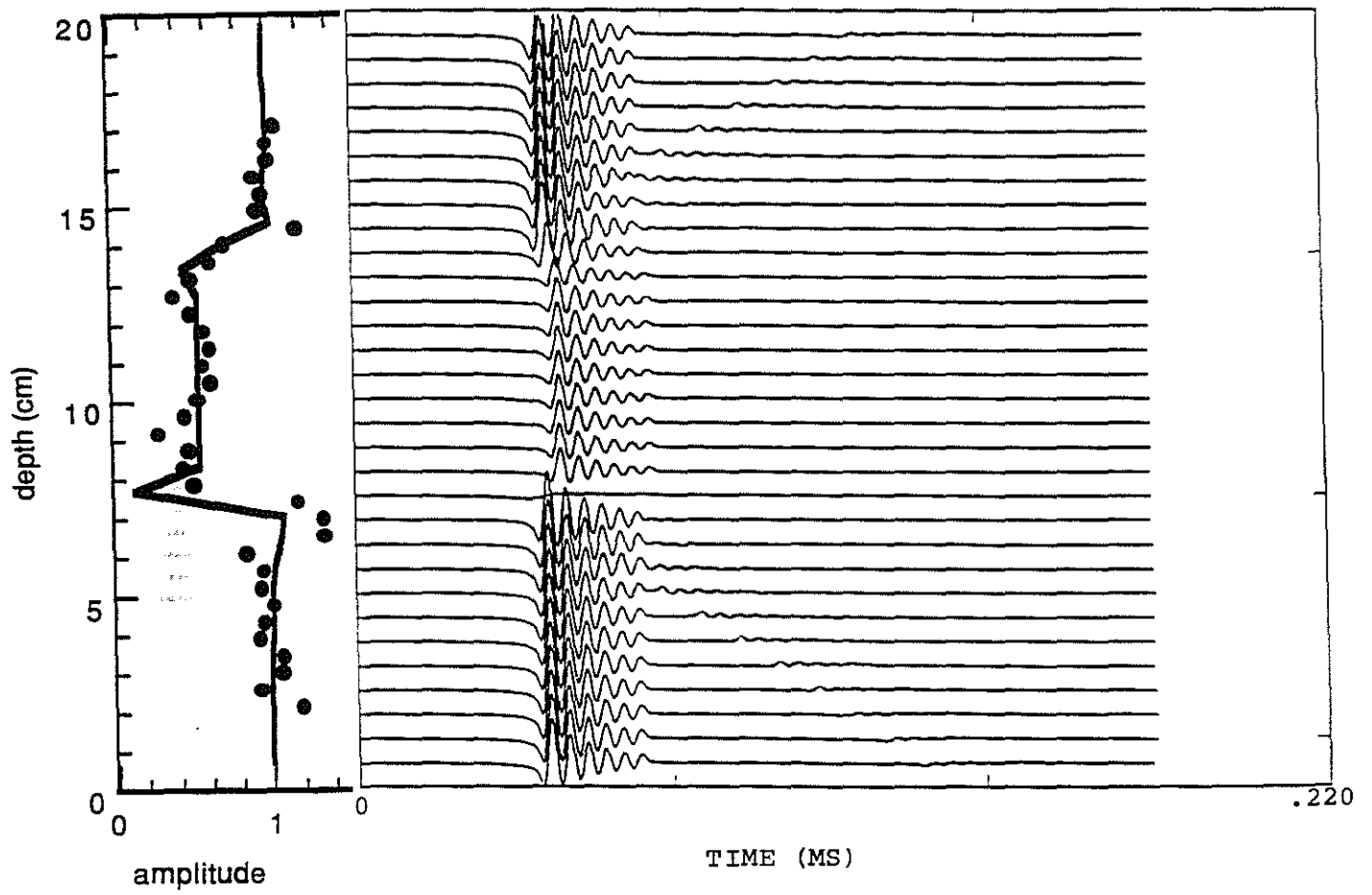


Figure 5: b) Synthetic waveforms (depth increment=0.75 cm) and amplitude log. For comparison, the experimental log (dots) is also plotted. The two logs agree very well.

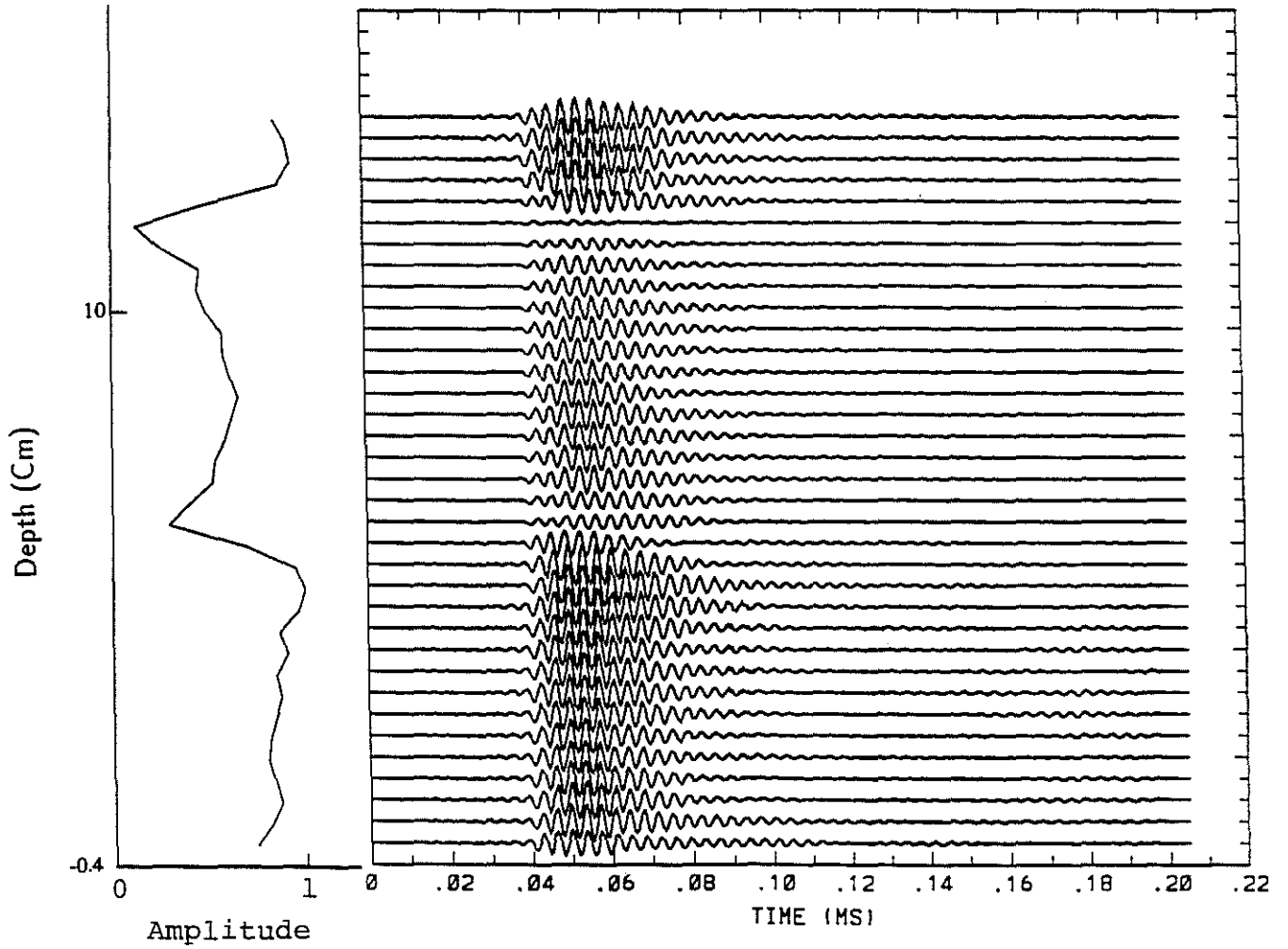


Figure 6: a) Amplitude log of Stoneley waves and waveforms (depth increment=0.4 cm) recorded in a permeable zone borehole model saturated with ethyl alcohol. The measured transmission coefficient is 0.59. The parameters of the permeable fracture zone are the same as in Figure 5a).

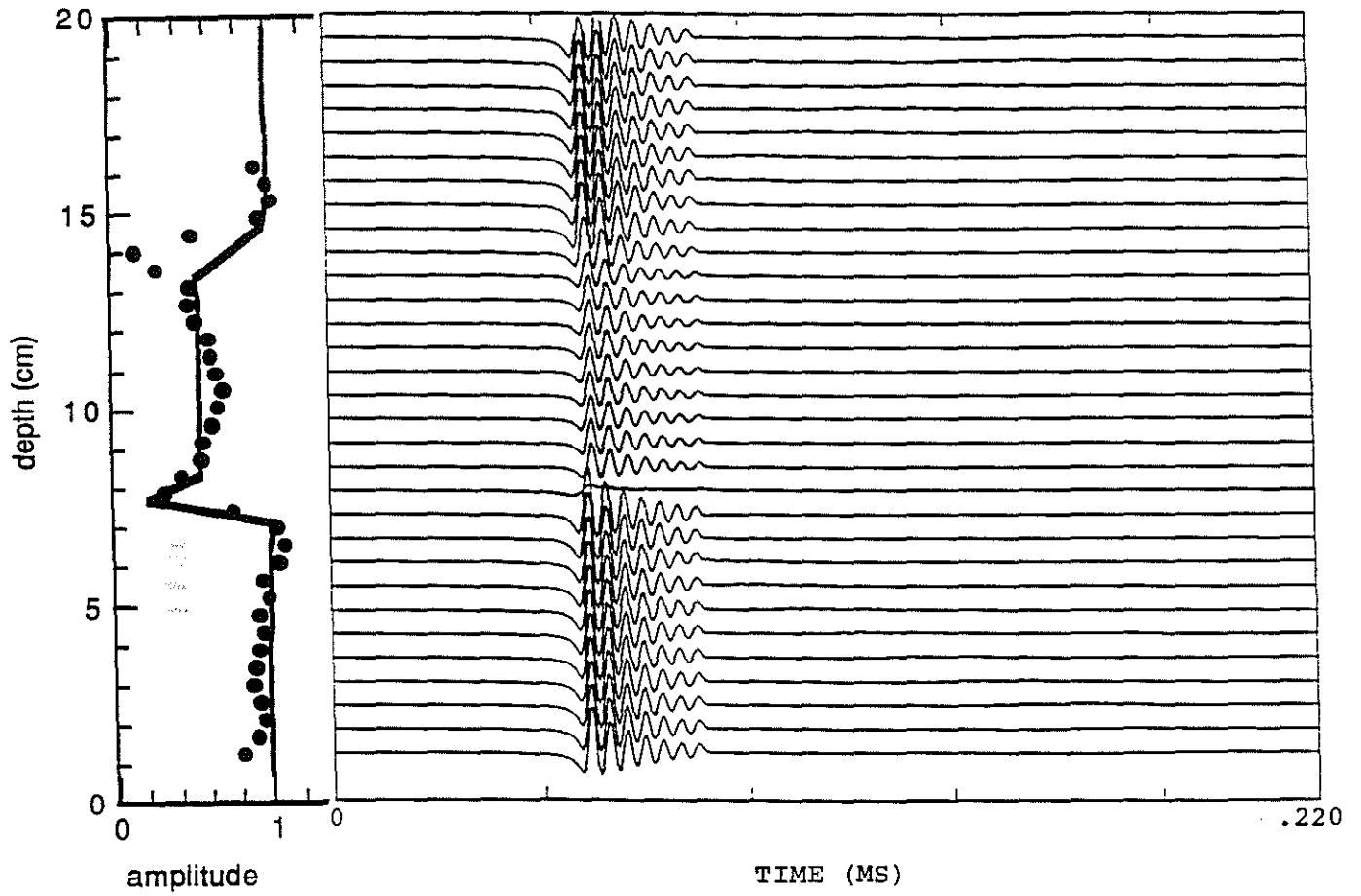


Figure 6: b) Synthetic waveforms (depth increment=0.75) and amplitude log across the permeable zone. The theory and experiment agree very well.

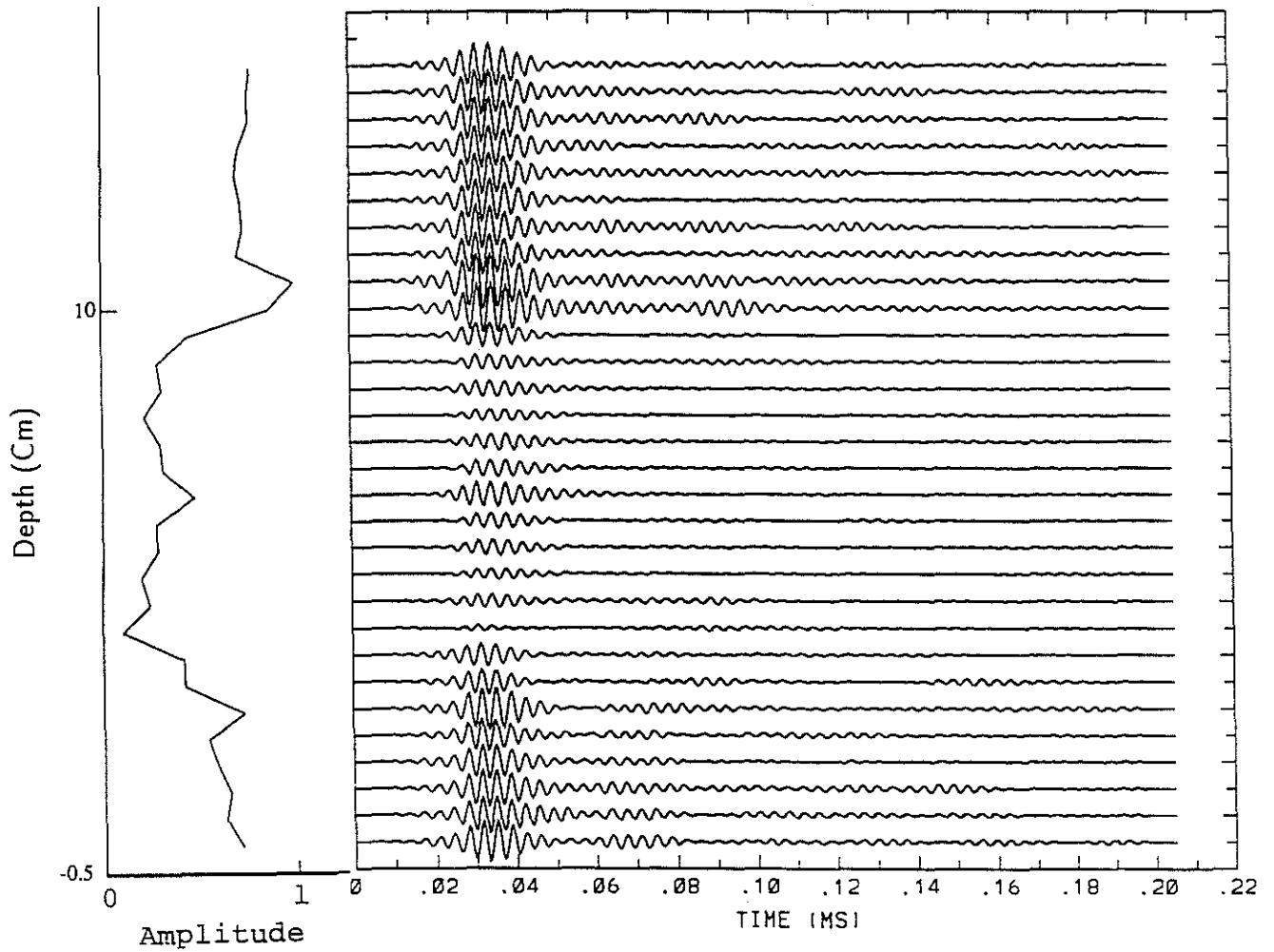


Figure 7: a) Amplitude log of Stoneley waves and waveforms (depth increment = 0.5 cm) recorded in a permeable zone model saturated with glycerol. The measured transmission coefficient is 0.43. Other parameters are the same as in Figure 5a).

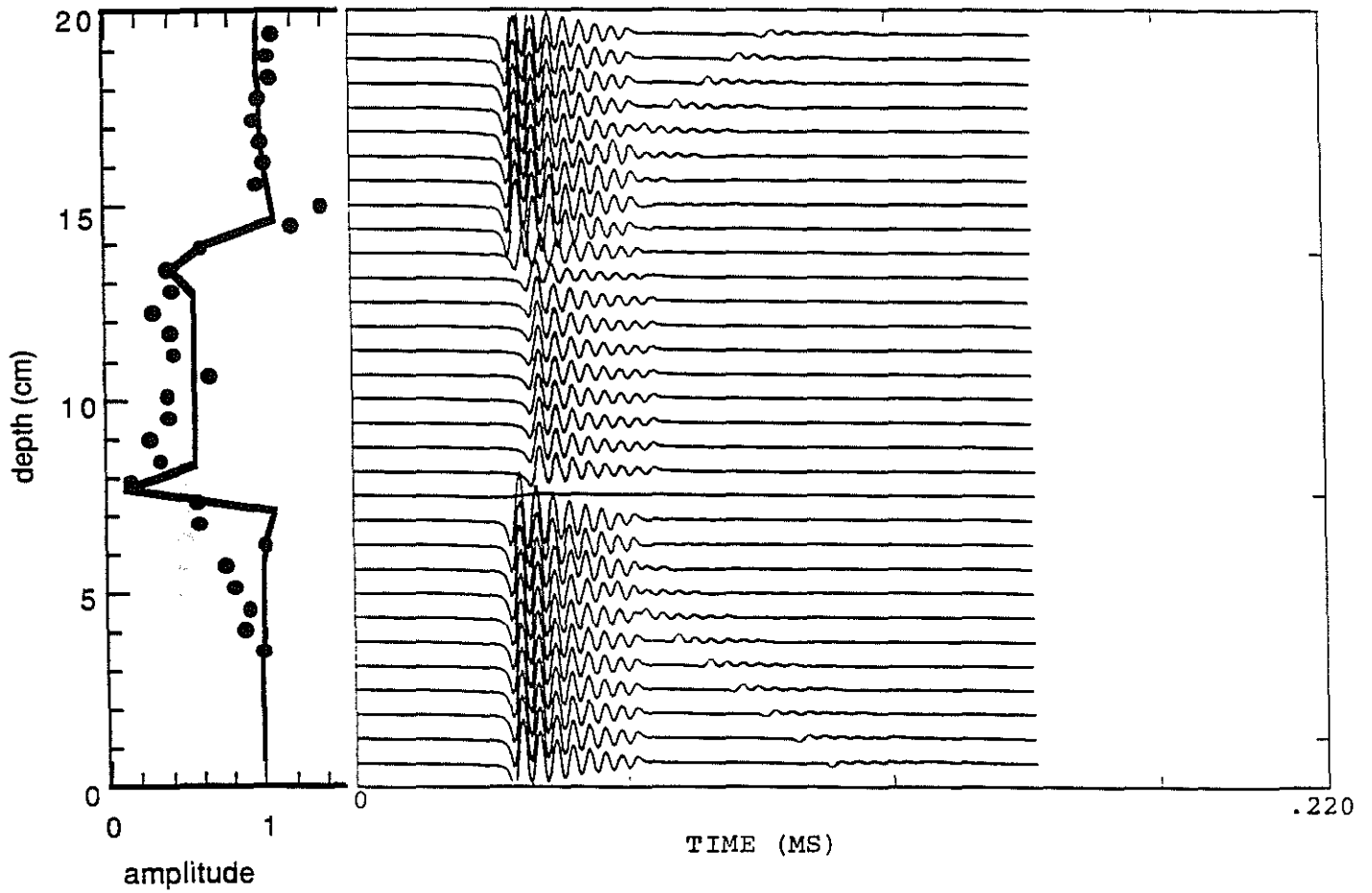


Figure 7: b) Synthetic waveforms and amplitude log across the permeable layer (depth increment=0.75 cm). In this very viscous saturant fluid case, the experiment exhibits more attenuation than the theory predicts.

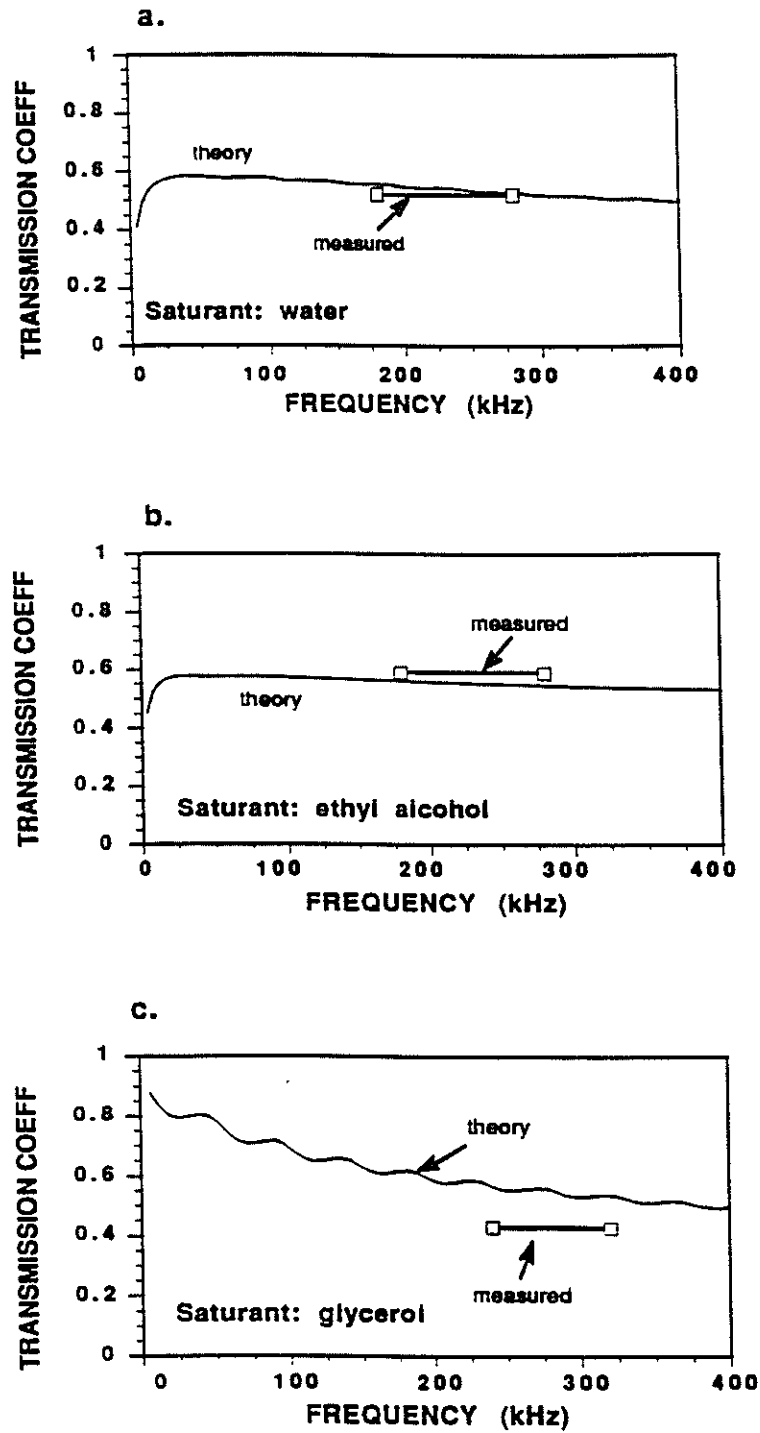


Figure 8: Comparison of theoretical and measured transmission coefficients in the frequency range of measurement for the three saturant fluids.